PHYSICAL REVIEW A VOLUME 49, NUMBER 4 APRIL 1994

Energy levels in Ar II

P. Quinet and P. Palmeri
Faculté des Sciences, Université de Mons-Hainaut, 15, rue de la Halle, B-7000 Mons, Belgium

E. Biémont*
Institut d'Astrophysique, Université de Liège, 5, Avenue de Cointe, B-4000 Liège, Belgium

J. W. Brault
National Solar Observatory, 950 North Cherry Avenue, P.O. Box 26732, Tucson, Arizona
(Received 3 August 1993)

The spectra of Cu, Mg, and V, produced by a hollow cathode with Ar and Ne as carrier gases, have been registered in the infrared region (1800–9000 cm^{-1}) with the Fourier-transform spectrometer at the National Solar Observatory on Kitt Peak. These spectra reveal the presence of three groups of lines around 1.8, 3.1, and 2.9 μm. Many of these emission lines have been identified as $3p^4(^3P)5f$-$6g$, $5g$-$6h$, $6g$-$7h$, $6h$-$7i$, and $6f$-$7g$ transitions in Ar II. From these observations, it has been possible to extend the term system of this ion and to determine the energies of approximately 70 new levels. More precisely, the $3p^4(^3P)6h$, $7h$, and $7i$ configurations have been analyzed.

PACS number(s): 32.30.Bv, 32.70.−n

I. INTRODUCTION

Since the publication of the *Atomic Energy Levels* [1], singly ionized argon, Ar II, has been the subject of a number of investigations. The energy levels have been thoroughly studied by Minnhagen and co-workers [2–8] and by Herzberg [9]. In particular a theoretical calculation of the Ar II $3p^4nf$ configurations ($n=4$–6) has been reported by Minnhagen and Svensson [8], their investigation including tables of eigenvectors and a discussion of the strong $(^3P_2)nf$ $[3]^o$ and $[4]^o$ $(J=7/2)$ mixing (the bracket notation is defined in detail in Sec. II). A comprehensive investigation of the Ar II spectrum was also published by Minnhagen [10] on the basis of observations in the spectral range 0.2–1.25 μm. His analysis has led to the determination of about 200 new energy levels including those belonging to the nf $(n=4$–$8)$ and ng $(n=5$–$8)$ configurations. Improved values of the levels of the $3s3p^6$ and $3p^4nl$ ($l=s$, p, and d) configurations were obtained from new measurements of the resonance lines and other ground-term combinations with the NBS 10.7-m vacuum spectrograph [11]. Interferometric measurements of Ar II wavelengths in the region 0.5–0.7 μm were reported by Norlén [12] with an estimated uncertainty on the wavelengths typically of the order of ±0.0004 Å. Further investigations are due to the same author [13] on the basis of interferometric measurements in the region 0.34–0.98 μm (water-cooled hollow cathode at a pressure of 0.2 torr[1]). 153 levels in Ar II, in particular, two $(^3P)5f$ and thirteen $(^3P)6g$ levels, were accurately redetermined, the uncertainty of the relative values varying from a few ten-thousandths to a few thousandths of a cm^{-1}.

The high resolution spectra registered by one of us (J.W.B.) using Fourier-transform spectroscopy (FTS) have extended the previous observations to the infrared region ($\lambda > 1.2$ μm). The spectra analyzed in the present investigation were observed during copper, magnesium, and vanadium hollow-cathode runs.

In this paper we present an analysis of three groups of lines appearing in the infrared at around 1.8, 3.1, and 2.9 μm respectively. These emission features have been identified as belonging to the $5f$-$6g$, $5g$-$6h$, $6g$-$7h$, $6h$-$7i$, and $6f$-$7g$ transition arrays of Ar II.

II. THE OBSERVATIONS

As was the case for previous observations [14–15] in the same spectral range, the spectra investigated were obtained with different hollow cathodes (Cu, Mg, and V) and the recordings were made in the 1800–9000 cm^{-1} region with the National Solar Observatory Fourier transform spectrometer [16,17]. Different sets of observations were obtained with Ne, Ar, He+Ar, and Ne+Ar as carrier gases and with a CaF_2 beam splitter. We give hereafter between parentheses, for each run, the source pressures of the different gases and the currents:

(a) V+Ar (0.98 torr, 0.46 A), V+Ne (2.02 torr, 0.51 A), V+He+Ar (1.1 torr of He, 1.0 torr of Ar, 0.40 A) in the region 2800–9000 cm^{-1}, V+Ne+Ar (2.4 torr of Ne, 0.05 torr of Ar, 0.37 A) in the range 1800–5800 cm^{-1};

(b) Cu+Ar (1.5 torr, 0.31 A) and Cu+Ne (2.6 torr, 0.60 A) in the spectral range 1800–5800 cm^{-1};

(c) Mg+Ar (0.65 torr, 0.34 A), Mg+Ne (1.28 torr, 0.38 A) in the region 3600–9000 cm^{-1}, Mg+Ne+Ar (0.74 torr of Ne, 0.012 torr of Ar, 0.18 A), Mg+He+Ar (1.68 torr of He, 0.53 torr of Ar, 0.35 A) in the spectral range 2800–9000 cm^{-1} and finally Mg+Ar (1.17 torr, 0.47 A) and Mg+Ar+Ne (1.0 torr of Ne, 1.17 torr of Ar,

[1] 1 torr = 133 Pa = 1.33 mbar.

1050-2947/94/49(4)/2446(7)/$06.00

0.51 A) in the region 1800–5800 cm^{-1}.

The lines of the carrier gases were sorted out of the recordings by comparison of the different spectra covering the same spectral region. The Ar lines of interest in this analysis appeared generally more intense in the V+Ar discharge in the region 1.76–1.87 μm and in the Cu+Ar discharge in the ranges 3.05–3.10 and 2.95–3.00 μm. This is not necessarily true in other spectral regions as illustrated on Fig. 1 showing a comparison between the V+Ne+Ar, Mg+Ar, and Cu+Ar spectra around 3245 cm^{-1}. Except in a few cases corresponding to broad line profiles or to very weak emission features for which the wave numbers were obtained by interpolation, a peak-finding computer program was used to generate automatically the positions of the lines. The preliminary observed wave numbers corresponding to the different sets of observations were calibrated (the wave-number scale being based on the internal spectrometer laser calibration) by means of a linear correction deduced from a comparison with the $4p$-$3d$ transitions of Ar I measured interferometrically by Norlén [13] between 4171 and 9023 cm^{-1}. This correction was typically a few 10^{-3} cm^{-1}. As pointed out previously [14,15], the wave numbers of the calibrated lines in the overlapping regions differ by a few 10^{-4} cm^{-1}, indicating an internal consistency of the observations superior to 10^{-3} cm^{-1}. The adequacy of the calibration procedure based on Norlén's wave numbers has been confirmed very recently by Whaling [18]: he calibrated his hollow-cathode spectra using accurate CO molecular lines and deduced Ar II energy levels in agreement with Norlén's values.

The air wavelengths (in μm), the vacuum wave numbers (in cm^{-1}), the observed relative intensities and the line identifications are given in Tables I–III for the Ar II transitions identified as $3p^4(^3P)5f$-$6g$ and $5g$-$6h$ (Table I), $6g$-$7h$ and $6h$-$7i$ (Table II) and $6f$-$7g$ (Table III) respectively. Except when otherwise indicated, the reported wave numbers are taken from the V+Ar and the Cu+Ar spectra. In the case of the Mg spectra, many lines of Ar II of interest here were blended.

According to Minnhagen [10], the observations of the Ar II spectrum show that LS coupling is valid for the deepest $3p^4ns$, np, and nd configurations whereas pair coupling is progressively better satisfied for higher l and n values. The level designations in Tables I to III are given according to the $J_C l$-coupling scheme. They are labeled according to the notation $3p^4(^{2S+1}L_{J_C})nl[K]_J$ where J_C is the total angular momentum quantum number of the electron core $3p^4\ ^3P$ level; K results from the coupling of the orbital angular momentum l of the valence electron to J_C and J is obtained through the addition of the spin of the valence electron to K.

Many of the wave numbers reported in Table I and some of them reported in Table II are expected to be accurate to the third decimal. For the other ones given in Tables II and III, the accuracy is reduced typically to 0.01 cm^{-1} due to very weak or broad profiles. The identifications were assessed by a comparison of the observed positions of the lines and their intensities with theoretical positions and oscillator strengths calculated with Cowan's computer code in the framework of the Relativistic Hartree-Fock (HFR) approximation [19]. The HFR oscillator strengths obtained in a monoconfigurational approximation for the $5g$-$6h$, $5f$-$6g$, $6h$-$7i$, $6g$-$7h$, and $6f$-$7g$ transition arrays are reported in Tables I–III. As illustrated in Fig. 2, this comparison was very helpful in a number of cases for disentangling the blends.

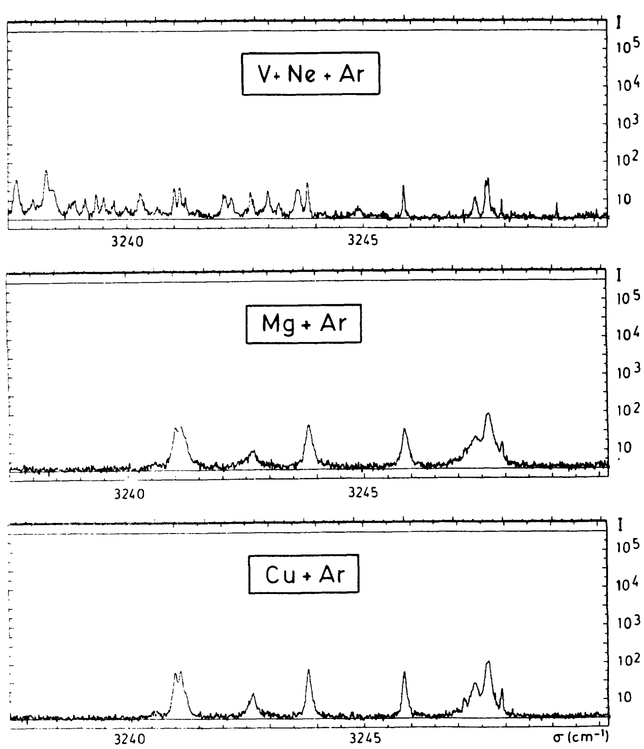

FIG. 1. Comparison of the V+Ne+Ar, Mg+Ar, and Cu+Ar spectra around 3245 cm^{-1}. The Ar II lines are clearly enhanced in the Cu and Mg spectra. The intensity I is plotted in a logarithmic scale.

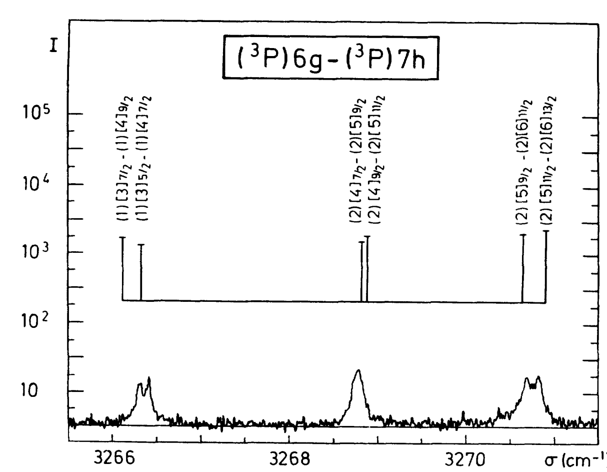

FIG. 2. Observed and calculated intensities for $6g$-$7h$ transitions of Ar II in the region 3266–3271 cm^{-1}. The differences between theoretical and experimental intensities for $\sigma = 3266.40$ cm^{-1} are due to a blend with the Ar II $3p^4(^3P)4d\ ^4P_{1/2}$-$3p^4(^3P)5p\ ^4P^o_{1/2}$ transition.

III. THE ENERGY LEVELS

The energy levels which have been deduced from our observations are reported in Table IV for the $(^3P)5f$, $5g$, $6g$, $6h$, $7h$, and $7i$ configurations. The ground state of Ar III is $3p^4\ ^3P_2$, and the energies of the parent terms $3p^4\ ^1D$ and $3p^4\ ^1S$ of Ar III are 14010.0 and 33265.7 cm^{-1} respectively [20]. As a consequence, the transitions originating from $(^1D)nl$ and $(^1S)nl$ levels ($n=6$–7, $l=g,h,i$) are not excited in the hollow-cathode discharge used in this work. Most of the $5f$ energy levels reported in Table IV were deduced through combinations with the accurate $6g$ terms as reported by Norlén [13]. The $(^3P_1)5f[3]^o_{7/2}$, $(^3P_1)5f[4]^o_{9/2}$, $(^3P_2)5f[4]^o_{9/2}$, and $(^3P_2)5f[5]^o_{11/2}$ level

TABLE I. Air wavelengths (in μm), observed wave numbers (in cm^{-1}), intensities, and oscillator strengths ($\log_{10}gf$) for $5f$-$6g$ and $5g$-$6h$ transitions in Ar II spectrum. The wave numbers have been measured on the V+Ar spectra. The intensity scale is referred to $\sigma=5382.129$ cm^{-1} ($I=1000$). The oscillator strengths are calculated with Cowan's HFR code [18] in a monoconfigurational approximation; only the gf values for the strongest (i.e., $\Delta K=1$, $\Delta J=1$, and $\Delta K=0$, $\Delta J=0$) transitions are given. The notations $(J_c)nl[K]_J$ have been adopted for $3p^4(^3P_{J_C})nl[K]_J$.

λ_{air} (μm)	σ_{obs} (cm^{-1})	Int.	Transition	$\log_{10}gf$
1.867 046	5 354.592	45	$(1)5g[4]_{7/2,9/2}$ -$(1)6h[4]^o_{7/2,9/2}$	$-0.29, -0.19$
1.864 626	5 361.541	245	$(2)5g[2]_{5/2}$ -$(2)6h[3]^o_{7/2}$	0.98
1.864 578	5 361.680	160	$(2)5g[2]_{3/2}$ -$(2)6h[3]^o_{5/2}$	0.83
1.863 940	5 363.515	80	$(2)5g[6]_{13/2}$ -$(2)6h[6]^o_{13/2}$	0.10
1.860 446	5 373.587	515	$(1)5g[4]_{7/2,9/2}$ -$(1)6h[5]^o_{9/2,11/2}$	1.11,1.20
1.857 494	5 382.129	1000	$(2)5g[6]_{11/2,13/2}$-$(2)6h[7]^o_{13/2,15/2}$	1.28,1.34
1.852 428	5 396.847	370	$(2)5g[3]_{7/2}$ -$(2)6h[4]^o_{9/2}$	1.07
1.852 393	5 396.949	270	$(2)5g[3]_{5/2}$ -$(2)6h[4]^o_{7/2}$	0.96
1.852 000	5 398.094	740	$(0)5g[4]_{7/2,9/2}$ -$(0)6h[5]^o_{9/2,11/2}$	1.13,1.22
1.848 947	5 407.009	470	$(1)5g[5]_{9/2}$ -$(1)6h[6]^o_{11/2}$	1.21
1.848 925	5 407.073	480	$(1)5g[5]_{11/2}$ -$(1)6h[6]^o_{13/2}$	1.29
1.847 08	5 412.48[a]	40	$(2)5g[3]_{7/2}$ -$(2)6h[3]^o_{7/2}$	0.11
1.847 04	5 412.60[a]	40	$(2)5g[3]_{5/2}$ -$(2)6h[3]^o_{5/2}$	-0.01
1.846 254	5 414.894	380	$(1)5g[3]_{7/2}$ -$(1)6h[4]^o_{9/2}$	1.12
1.846 215	5 415.008	290	$(1)5g[3]_{5/2}$ -$(1)6h[4]^o_{7/2}$	1.01
1.843 855	5 421.939	850	$(2)5g[4]_{7/2,9/2}$ -$(2)6h[5]^o_{9/2,11/2}$	1.08,1.17
1.842 749	5 425.192[b]	400	$(2)5g[5]_{9/2}$ -$(2)6h[6]^o_{11/2}$	1.18
1.842 741	5 425.218	490	$(2)5g[5]_{11/2}$ -$(2)6h[6]^o_{13/2}$	1.26
1.840 382	5 432.171	110	$(2)5g[4]_{7/2,9/2}$ -$(2)6h[4]^o_{7/2,9/2}$	0.18,0.28
1.829 451	5 464.629	80	$(2)5f[1]^o_{3/2}$ -$(2)6g[2]_{5/2}$	0.62
1.824 926	5 478.177	40	$(2)5f[1]^o_{1/2}$ -$(2)6g[2]_{3/2}$	0.36
1.816 58	5 503.35[a]	40	$(2)5f[5]^o_{9/2}$ -$(2)6g[5]_{9/2}$	-0.10
1.815 638	5 506.203	125	$(1)5f[3]^o_{5/2}$ -$(1)6g[4]_{7/2}$	0.80
1.812 469	5 515.831	150	$(1)5f[3]^o_{7/2}$ -$(1)6g[4]_{9/2}$	0.92
1.805 115	5 538.300	220	$(2)5f[5]^o_{9/2}$ -$(2)6g[6]_{11/2}$	1.02
1.803 864	5 542.142	235	$(2)5f[5]^o_{11/2}$ -$(2)6g[6]_{13/2}$	1.10
1.800 969	5 551.050	135	$(2)5f[2]^o_{5/2}$ -$(2)6g[3]_{7/2}$	0.73
1.796 011	5 566.375	155	$(0)5f[3]^o_{5/2}$ -$(0)6g[4]_{7/2}$	0.84
1.793 616	5 573.808	100	$(2)5f[2]^o_{3/2}$ -$(2)6g[3]_{5/2}$	0.58
1.793 547	5 574.022	180	$(0)5f[3]^o_{7/2}$ -$(0)6g[4]_{9/2}$	0.95
1.791 751	5 579.610	30	$(2)5f[2]^o_{5/2}$ -$(2)6g[2]_{5/2}$	0.00
1.790 532	5 583.408	185	$(1)5f[4]^o_{7/2}$ -$(1)6g[5]_{9/2}$	0.94
1.785 364	5 599.569	205	$(1)5f[4]^o_{9/2}$ -$(1)6g[5]_{11/2}$	1.03
1.784 501	5 602.277	25	$(2)5f[2]^o_{3/2}$ -$(2)6g[2]_{3/2}$	-0.10
1.783 509	5 605.394	150	$(1)5f[2]^o_{5/2}$ -$(1)6g[3]_{7/2}$	0.81
1.781 265	5 612.455	25	$(1)5f[4]^o_{7/2}$ -$(1)6g[4]_{7/2}$	-0.34
1.781 027	5 613.204	125	$(2)5f[3]^o_{7/2}$ -$(2)6g[4]_{9/2}$	0.41
1.778 182	5 622.186	100	$(1)5f[2]^o_{3/2}$ -$(1)6g[3]_{5/2}$	0.66
1.775 157	5 631.765	150	$(2)5f[3]^o_{5/2}$ -$(2)6g[4]_{7/2}$	0.72
1.774 449	5 634.014	25	$(2)5f[3]^o_{7/2}$ -$(2)6g[3]_{7/2}$	-0.08
1.768 653	5 652.477	35	$(2)5f[3]^o_{5/2}$ -$(2)6g[3]_{5/2}$	0.14
1.767 355	5 656.629	110	$(2)5f[4]^o_{7/2}$ -$(2)6g[5]_{9/2}$	0.50
1.766 847	5 658.256	90	$(2)5f[4]^o_{7/2}$ -$(2)6g[4]_{7/2}$	-0.54
1.763 255	5 669.781	215	$(2)5f[4]^o_{9/2}$ -$(2)6g[5]_{11/2}$	0.99
1.762 710	5 671.536	45	$(2)5f[4]^o_{9/2}$ -$(2)6g[4]_{9/2}$	0.13

[a]Not directly given by the peak-finding program but interpolated (see the text).

[b]Not clearly seen: appears in the wing of the Ar I $3d[3/2]^o_1$-$4p'[1/2]_0$ transition at $\sigma=5425.112$ cm^{-1}.

TABLE II. Air wavelengths (in μm), observed wave numbers (in cm^{-1}), intensities and oscillator strengths ($\log_{10}gf$) for $6g$-$7h$ and $6h$-$7i$ transitions in Ar II spectrum. The wave numbers have been measured on Cu+Ar spectra; wave numbers given with two decimals correspond to broad profiles or weak lines. The intensity scale is referred to $\sigma=3247.638$ cm^{-1} ($I=1000$). The oscillator strengths are calculated with Cowan's HFR [18] code in a monoconfigurational approximation. The gf values for the strongest (i.e., $\Delta K=+1, \Delta J=+1$ and $\Delta K=0, \Delta J=0$) transitions only are given. For the transition notation, see the caption to Table I.

λ_{air} (μm)	σ_{obs} (cm^{-1})	Int.	Transition	$\log_{10}gf$
3.096 035	3 229.057[a]	60	$(2)6h\,[7]^{o}_{13/2,15/2}$-$(2)7i\,[7]_{13/2,15/2}$	0.05,0.11
3.093 890	3 231.30[b]	240	$(2)6h\,[3]^{o}_{5/2,7/2}$ -$(2)7i\,[4]_{7/2,9/2}$	1.08,1.19
3.091 3	3 234.0[c]		$(1)6h\,[5]^{o}_{9/2,11/2}$ -$(1)7i\,[6]_{11/2,13/2}$	1.29,1.36
3.089 7	3 235.7[d]	100	$(2)6g\,[2]_{3/2,5/2}$ -$(2)7h\,[3]^{o}_{5/2,7/2}$	0.78,0.93
3.089 409	3 235.983	650	$(2)6h\,[7]^{o}_{13/2,15/2}$-$(2)7i\,[8]_{15/2,17/2}$	1.43,1.49
3.084 629	3 240.996	560	$(2)6h\,[4]^{o}_{7/2,9/2}$ -$(2)7i\,[5]_{9/2,11/2}$	1.18,1.27
3.084 521	3 241.111	650	$(0)6h\,[5]^{o}_{9/2,11/2}$ -$(0)7i\,[6]_{11/2,13/2}$	1.30,1.38
3.083 08	3 242.63	150	$(1)6g\,[4]_{7/2,9/2}$ -$(1)7h\,[5]^{o}_{9/2,11/2}$	1.06,1.15
3.081 952	3 243.812	650	$(1)6h\,[6]^{o}_{11/2,13/2}$-$(1)7i\,[7]_{13/2,15/2}$	1.37,1.43
3.080 020	3 245.847	560	$(1)6h\,[4]^{o}_{7/2,9/2}$ -$(1)7i\,[5]_{9/2,11/2}$	1.21,1.30
3.078 821	3 247.111	100	$(2)6h\,[6]^{o}_{11/2,13/2}$-$(2)7i\,[6]_{11/2,13/2}$	0.21,0.28
3.078 58	3 247.37	270	$(2)6g\,[6]_{11/2,13/2}$-$(2)7h\,[7]^{o}_{13/2,15/2}$	1.23,1.29
3.078 360	3 247.597	870	$(2)6h\,[6]^{o}_{11/2}$ -$(2)7i\,[7]_{13/2}$	1.35
			$(2)6h\,[5]^{o}_{9/2,11/2}$ -$(2)7i\,[6]_{11/2,13/2}$	1.27,1.34
3.078 321	3 247.638	1000	$(2)6h\,[6]^{o}_{13/2}$ -$(2)7i\,[7]_{15/2}$	1.41
3.074 92	3 251.23	60	$(2)6h\,[5]^{o}_{9/2,11/2}$ -$(2)7i\,[5]_{9/2,11/2}$	0.20,0.28
3.071 88	3 254.45	140	$(2)6g\,[3]_{7/2}$ -$(2)7h\,[4]^{o}_{9/2}$	1.02
3.071 83	3 254.50	140	$(2)6g\,[3]_{5/2}$ -$(2)7h\,[4]^{o}_{7/2}$	0.91
3.069 73	3 256.73	120	$(0)6g\,[4]_{7/2}$ -$(0)7h\,[5]^{o}_{9/2}$	1.08
3.069 57	3 256.90	130	$(0)6g\,[4]_{9/2}$ -$(0)7h\,[5]^{o}_{11/2}$	1.17
3.065 17	3 261.57	180	$(1)6g\,[5]_{9/2}$ -$(1)7h\,[6]^{o}_{11/2}$	1.16
3.065 12	3 261.63	190	$(1)6g\,[5]_{11/2}$ -$(1)7h\,[6]^{o}_{13/2}$	1.24
3.060 73	3 266.30	130	$(1)6g\,[3]_{7/2}$ -$(1)7h\,[4]^{o}_{9/2}$	1.07
3.060 64	3 266.40[e]		$(1)6g\,[3]_{5/2}$ -$(1)7h\,[4]^{o}_{7/2}$	0.96
3.058 41	3 268.78	200	$(2)6g\,[4]_{7/2,9/2}$ -$(2)7h\,[5]^{o}_{9/2,11/2}$	1.03,1.11
3.056 62	3 270.70	150	$(2)6g\,[5]_{9/2}$ -$(2)7h\,[6]^{o}_{11/2}$	1.12
3.056 49	3 270.83	180	$(2)6g\,[5]_{11/2}$ -$(2)7h\,[6]^{o}_{13/2}$	1.21

[a]Measured on the Mg+Ar spectrum.
[b]Measured on the V+Ne+Ar spectrum.
[c]Not clearly seen: blended with the Ar I $3d\,[5/2]^{o}_{2}$-$5p\,[1/2]_{1}$ transition at $\sigma=3234.038$ cm^{-1}.
[d]Blended with the line at $\sigma=3235.983$ cm^{-1}.
[e]Blended with the $(^3P)4d\ ^4P^{o}_{1/2}$-$(^3P)5p\ ^4P_{1/2}$ Ar II transition at $\sigma=3266.409$ cm^{-1}.

TABLE III. Air wavelengths (in μm), observed wave numbers (in cm^{-1}), intensities and oscillator strengths ($\log_{10}gf$) for $6f$-$7g$ transitions in Ar II spectrum. The wave numbers have been measured on the Cu+Ar spectra, and are quoted with two decimals because most of these weak emission lines show broad profiles. The intensity scale is referred to $\sigma=3247.638$ cm^{-1} ($I=1000$). The oscillator strengths are calculated with Cowan's HFR code (monoconfigurational approximation) [18]. The notations $(J_c)nl\,[K]_J$ have been adopted for $3p^4(^3P_{J_C})nl\,[K]_J$.

λ_{air} (μm)	σ_{obs} (cm^{-1})	Int.	Transition	$\log_{10}gf$
3.004 12	3 327.85	60	$(1)6f\,[3]^{o}_{5/2}$ -$(1)7g\,[4]_{7/2}$	0.75
2.997 19	3 335.55	75	$(1)6f\,[3]^{o}_{7/2}$ -$(1)7g\,[4]_{9/2}$	0.87
2.987 58	3 346.28	130	$(2)6f\,[5]^{o}_{9/2}$ -$(2)7g\,[6]_{11/2}$	0.97
2.987 31	3 346.58	75	$(2)6f\,[2]^{o}_{5/2}$ -$(2)7g\,[3]_{7/2}$	0.67
2.985 02	3 349.15	150	$(2)6f\,[5]^{o}_{11/2}$-$(2)7g\,[6]_{13/2}$	1.05
2.974 69	3 360.78	50	$(2)6f\,[2]^{o}_{3/2}$ -$(2)7g\,[3]_{5/2}$	0.53
2.971 05	3 364.90	90	$(0)6f\,[3]^{o}_{5/2}$ -$(0)7g\,[4]_{7/2}$	0.79
2.966 20	3 370.40	90	$(0)6f\,[3]^{o}_{7/2}$ -$(0)7g\,[4]_{9/2}$	0.90
2.964 35	3 372.50	100	$(1)6f\,[4]^{o}_{7/2}$ -$(1)7g\,[5]_{9/2}$	0.89
2.955 47	3 382.63	75	$(2)6f\,[3]^{o}_{7/2}$ -$(2)7g\,[4]_{9/2}$	0.63
2.953 07	3 385.38	100	$(1)6f\,[4]^{o}_{9/2}$ -$(1)7g\,[5]_{11/2}$	0.99
2.950 35	3 388.50	90	$(1)6f\,[2]^{o}_{5/2}$ -$(1)7g\,[3]_{7/2}$	0.76
2.943 88	3 395.95	60	$(2)6f\,[3]^{o}_{5/2}$ -$(2)7g\,[4]_{7/2}$	0.66
2.938 38	3 402.30	50	$(1)6f\,[2]^{o}_{3/2}$ -$(1)7g\,[3]_{5/2}$	0.62
2.929 78	3 412.30	50	$(2)6f\,[4]^{o}_{7/2}$ -$(2)7g\,[5]_{9/2}$	0.68
2.922 75	3 420.50	130	$(2)6f\,[4]^{o}_{9/2}$ -$(2)7g\,[5]_{11/2}$	0.94

values were obtained from $5f$-$6g$ combinations with $(^3P_1)6g[4]_{9/2}$, $(^3P_1)6g[5]_{11/2}$, $(^3P_2)6g[5]_{11/2}$, and $(^3P_2)6g[6]_{13/2}$ levels taken from Minnhagen's analysis [10] corrected to include an upward shift of 0.08 cm^{-1} [11]. The refined value of $(^3P_2)6g[6]_{11/2}$ (not observed in Norlén's work) has been established from the observation of the $(^3P_2)5f[5]^o_{9/2}$-$(^3P_2)6g[6]_{11/2}$ transition with the $5f$ energy level taken from Ref. [13]. The $3p^4(^3P)7h$ level values were deduced from the $6g$-$7h$ wave numbers reported in Table II and the $6g$ levels as given in Table IV. The present $6h$ and $7i$ energy levels are based on combinations $5g$-$6h$ and $6h$-$7i$ with the $5g$ values of Minnhagen [10] in the present energy scale [11]. The wave numbers of Table III ($6f$-$7g$) were not used for refining level values [10,11,13] because all these weak emission lines show rather broad profiles.

It should be emphasized that the accuracy of the FTS measurements in principle allows the establishment of more accurate energy level values than those given in Table IV. The accuracy of the levels reported here (± 0.01 cm^{-1}) is limited by broad or unresolved profiles caused by close or unresolved pairs of levels. A further refinement would also require a detailed consideration of Stark and pressure shifts which are likely to be non-negligible for the high-n and -l Rydberg states analyzed in the present work. It has been shown in a recent publication on Ne I [21] that the inclusion of van der Waals pressure shift deduced from the standard formula does not necessarily improve the agreement between measured and theoretical energy levels. Ideally one should take spectra at different argon pressures and extrapolate the line positions to zero pressure. The present spectra how-

TABLE IV. New or refined energy level values for $(^3P)5f$, $5g$, $6g$, $6h$, $7h$, and $7i$ configurations in Ar II. The levels have not been corrected for Stark and pressure shifts (see the text). r, the value of Ref. [10] has been refined; c, the value of Ref. [10] increased by 0.08 cm^{-1} according to Ref. [11]; n, taken from Ref. [13].

Design.	J	Level	Design.	J	Level
	$5f$			$5g$	
$(^3P_0)[3]$	5/2	206 631.72 r	$(^3P_0)[4]$	7/2	206 819.39 c
	7/2	206 623.91 r		9/2	206 819.40 c
$(^3P_1)[2]$	3/2	206 103.47 r	$(^3P_1)[3]$	5/2	206 336.95 c
	5/2	206 120.38 r		7/2	206 337.08 c
$(^3P_1)[3]$	5/2	206 255.27 r	$(^3P_1)[4]$	7/2	206 397.38 c
	7/2	206 245.63 r		9/2	206 397.37 c
$(^3P_1)[4]$	7/2	206 149.02 r	$(^3P_1)[5]$	9/2	206 347.96 c
	9/2	206 132.77 r		11/2	206 347.91 c
$(^3P_2)[1]$	1/2	205 180.45 r	$(^3P_2)[2]$	3/2	205 300.94 c
	3/2	205 194.10 r		5/2	205 301.08 c
$(^3P_2)[2]$	3/2	205 056.33 r	$(^3P_2)[3]$	5/2	205 250.01 c
	5/2	205 079.13 r		7/2	205 250.11 c
$(^3P_2)[3]$	5/2	204 977.65 r	$(^3P_2)[4]$	7/2	205 214.79 c
	7/2	204 996.1715 n		9/2	205 214.79 c
$(^3P_2)[4]$	7/2	204 951.13 r	$(^3P_2)[5]$	9/2	205 212.10 c
	9/2	204 937.85 r		11/2	205 211.97 c
$(^3P_2)[5]$	9/2	205 104.427 n	$(^3P_2)[6]$	11/2	205 273.67 c
	11/2	205 100.54 r		13/2	205 273.68 c
	$6g$			$6h$	
$(^3P_0)[4]$	7/2	212 198.0935 n	$(^3P_0)[5]$	9/2	212 217.49
	9/2	212 197.936 n		11/2	212 217.49
$(^3P_1)[3]$	5/2	211 725.657 n	$(^3P_1)[4]$	7/2	211 751.96
	7/2	211 725.7716 n		9/2	211 751.97
$(^3P_1)[4]$	7/2	211 761.4686 n	$(^3P_1)[5]$	9/2	211 770.96
	9/2	211 761.46 c		11/2	211 770.96
$(^3P_1)[5]$	9/2	211 732.4322 n	$(^3P_1)[6]$	11/2	211 754.97
	11/2	211 732.34 c		13/2	211 754.98
$(^3P_2)[2]$	3/2	210 658.631 n	$(^3P_2)[3]$	5/2	210 662.62
	5/2	210 658.7305 n		7/2	210 662.62
$(^3P_2)[3]$	5/2	210 630.142 n	$(^3P_2)[4]$	7/2	210 646.96
	7/2	210 630.1836 n		9/2	210 646.96
$(^3P_2)[4]$	7/2	210 609.4122 n	$(^3P_2)[5]$	9/2	210 636.73
	9/2	210 609.3762 n		11/2	210 636.73
$(^3P_2)[5]$	9/2	210 607.7560 n	$(^3P_2)[6]$	11/2	210 637.29[a]
	11/2	210 607.63 c		13/2	210 637.19
$(^3P_2)[6]$	11/2	210 642.73 r	$(^3P_2)[7]$	13/2	210 655.81
	13/2	210 642.68 c		15/2	210 655.81

TABLE I. (*Continued*).

Design.	J	Level	Design.	J	Level
	$7h$			$7i$	
$(^3P_0)[5]$	9/2	215 454.82	$(^3P_0)[6]$	11/2	215 458.60
	11/2	215 454.84		13/2	215 458.60
$(^3P_1)[4]$	7/2	214 992.06	$(^3P_1)[5]$	9/2	214 997.82
	9/2	214 992.07		11/2	214 997.82
$(^3P_1)[5]$	9/2	215 004.09	$(^3P_1)[6]$	11/2	215 005.0[b]
	11/2	215 004.09		13/2	215 005.0[b]
$(^3P_1)[6]$	11/2	214 994.00	$(^3P_1)[7]$	13/2	214 998.79
	13/2	214 993.97		15/2	214 998.79
$(^3P_2)[3]$	5/2	213 894.4[b]	$(^3P_2)[4]$	7/2	213 893.92
	7/2	213 894.4[b]		9/2	213 893.92
$(^3P_2)[4]$	7/2	213 884.64	$(^3P_2)[5]$	9/2	213 887.96
	9/2	213 884.63		11/2	213 887.96
$(^3P_2)[5]$	9/2	213 878.18	$(^3P_2)[6]$	11/2	213 884.32[c]
	11/2	213 878.17		13/2	213 884.32[c]
$(^3P_2)[6]$	11/2	213 878.46	$(^3P_2)[7]$	13/2	213 884.89[a]
	13/2	213 878.46		15/2	213 884.83
$(^3P_2)[7]$	13/2	213 890.08	$(^3P_2)[8]$	15/2	213 891.79
	15/2	213 890.08		17/2	213 891.79

[a]Has larger uncertainty because the line $(^3P_2)5g\,[5]_{9/2}$-$(^3P_2)6h\,[6]^o_{11/2}$ is not clearly seen (see Table I).
[b]Energy levels deduced from unresolved blends (see Table II).
[c]Interpolated value (see the text).

ever were taken for spectral analysis of magnesium, copper, and vanadium with neon and argon as carrier gases. Consequently the pressure shifts corrections were not further considered here. Similarly the electric field present in the discharge could lead to Stark shifts of a few 10^{-3} cm^{-1} with either sign [21]. Their detailed evaluation however, which would require knowledge of the electric field strength, is very uncertain and consequently the removal of the Stark contribution from the level values was not attempted in the present work.

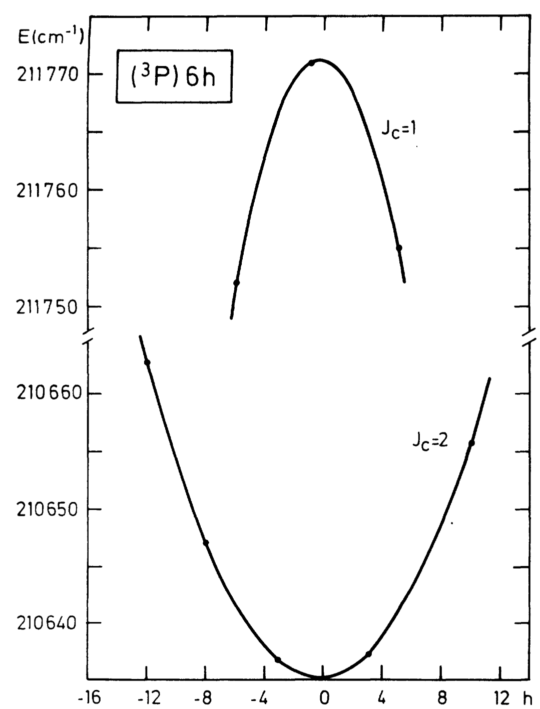

FIG. 3. Energies of $3p^4(^3P)6h$ levels plotted as a function of $h=\frac{1}{2}[K(K+1)-J_c(J_c+1)-l(l+1)]$. The curves are parabolas fitted to the experimental points.

The validity of the jK coupling has been verified by calculating with Cowan's computer code [19] the corresponding eigenvector compositions. These have been found to be very close to 100% for all the levels except $(^3P_2)5f\,[3]^o_{7/2}$ and $(^3P_2)5f\,[4]^o_{7/2}$ for which strong mixing occurs (see also Ref. [8]). In addition, the $6h$, $7h$, and $7i$ levels appear in closely spaced pairs well described by the jK coupling but with two components not or hardly separated on the spectra. If the splitting is neglected, the structure of $6h$, $7h$, and $7i$ configurations in jK coupling can be described by the so-called quadrupolar approximation [22]; the structure of such configurations was discussed by Racah [23,24] in terms of the quadrupole interaction between the core and the valence electron charge distributions. In pure jK coupling, the energies of a pair of levels (for a given J_C) should fall on a parabola when plotted against $h=\frac{1}{2}[K(K+1)-J_C(J_C+1)-l(l+1)]$ where l is associated with $6h$, $7h$, or $7i$ electrons. This approximation is nicely verified in the three cases. The example of $6h$ is illustrated in Fig. 3. Moreover, from these curves, it was possible to interpolate the values of $(^3P_2)7i\ [6]$ levels. For these levels in fact the $(^3P_2)6h\,[5]^o$-$(^3P_2)7i\ [6]$ transition is not clearly seen because it appears in the wing of the $3d\,[5/2]_2$-$5p\,[1/2]^o_1$ Ar I line at $\sigma=3234.038$ cm^{-1}.

IV. CONCLUSIONS

The energy levels of the Ar II $(^3P)6g$, $6h$, $7h$, and $7i$ configurations have been established on the basis of FTS infrared observations of Cu, Mg, and V spectra. It has been shown that the level structure of these configurations is well described in the pair-coupling approximation with small or unresolved pair splittings and the "quadrupolar" approximation has been found to provide an excellent description of the level structure of these configurations.

ACKNOWLEDGMENTS

Financial support from the Belgian FRFC, FNRS, and IRSIA is acknowledged. It is a pleasure also to thank Dr. J. E. Hansen (Amsterdam) for providing us with some output of Cowan's computer code and W. Whaling (Caltech) for sending some information concerning the calibration of his hollow-cathode spectra. The National Optical Astronomy Observations are operated by the Association of Universities for Research in Astronomy, Inc., under cooperative agreement with the National Science Foundation.

*Also at the Institut de Physique Nucléaire Expérimentale, Université de Liège, Sart Tilman, B-4000 Liège, Belgium.

[1] C. E. Moore, *Atomic Energy Levels,* NBS Circ. No. 467, Vol. 1 (1949); NSRDS-NBS **35**, Vol. 1 (Washington, D.C., 1971).
[2] L. Minnhagen, Ark. Fys. **14**, 123 (1958).
[3] L. Minnhagen, Ark. Fys. **14**, 483 (1958).
[4] L. Minnhagen, Ark. Fys. **18**, 97 (1960).
[5] L. Minnhagen and L. Stigmark, Ark. Fys. **8**, 471 (1954).
[6] L. Minnhagen and L. Stigmark, Ark. Fys. **13**, 27 (1957).
[7] L. Minnhagen, B. Petersson, and L. Stigmark, Ark. Fys. **16**, 541 (1960).
[8] L. Minnhagen and H. Svensson, Ark. Fys. **34**, 71 (1967).
[9] G. Herzberg, Proc. R. Soc. A **248**, 309 (1958).
[10] L. Minnhagen, Ark. Fys. **25**, 203 (1963).
[11] L. Minnhagen, J. Opt. Soc. Am. **61**, 1257 (1971).
[12] G. Norlén, Ark. Fys. **35**, 119 (1967).
[13] G. Norlén, Phys. Scr. **8**, 249 (1973).
[14] E. Biémont and J. W. Brault, Phys. Scr. **35**, 286 (1987).
[15] E. Biémont and J. W. Brault, Phys. Scr. **34**, 751 (1986).
[16] J. W. Brault, J. Opt. Soc. Am. **66**, 1081 (1976).
[17] J. W. Brault, Mem. Oss. Astron. Arcetri **106**, 33 (1979).
[18] W. Whaling (private communication).
[19] R. D. Cowan, in *The Theory of Atomic Structure and Spectra* (University of California Press, Berkeley, 1981).
[20] J. E. Hansen and W. Persson, J. Phys. B **20**, 693 (1987).
[21] E. S. Chang, W. G. Schoenfeld, E. Biémont, P. Quinet, and P. Palmeri, Phys. Scr. (to be published).
[22] Z. B. Goldschmidt, J. Phys. B **14**, 615 (1981).
[23] G. Racah, J. Opt. Soc. Am. **50**, 408 (1960).
[24] G. Racah, Phys. Rev. **61**, 537 (1942).